The Plant Cell, Vol. 17, 1994–2008, July 2005, www.plantcell.org

The Recessive Epigenetic *swellmap* Mutation Affects the Expression of Two Step II Splicing Factors Required for the Transcription of the Cell Proliferation Gene *STRUWWELPETER* and for the Timing of Cell Cycle Arrest in the Arabidopsis Leaf

Nicole K. Clay and Timothy Nelson[1]

Department of Molecular, Cellular, and Developmental Biology, Yale University, New Haven, Connecticut 06520-8104

Generally, cell division can be uncoupled from multicellular development, but more recent evidence suggests that cell cycle progression and arrest is coupled to organogenesis and growth. We describe a recessive mutant, *swellmap* (*smp*), with reduced organ size and cell number. This defect is partially compensated for by an increase in final cell size. The mutation causes a precocious arrest of cell proliferation in the organ primordium and possibly reduces the rate of cell division there. The mutation proved to be an epigenetic mutation (renamed *smp^{epi}*) that defined a single locus, *SMP1*, but affected the expression of both *SMP1* and a second very similar gene, *SMP2*. Both genes encode CCHC zinc finger proteins with similarities to step II splicing factors involved in 3′ splice site selection. Genetic knockouts demonstrate that the genes are functionally redundant and essential. *SMP1* expression is associated with regions of cell proliferation. Overexpression of *SMP1* produced an increase in organ cell number and a partial decrease in cell expansion. The *smp^{epi}* mutation does not affect expression of eukaryotic cell cycle regulator genes *CYCD3;1* and *CDC2A* but affects expression of the cell proliferation gene *STRUWWELPETER* (*SWP*) whose protein has similarities to Med150/Rgr1-like subunits of the Mediator complex required for transcriptional activation. Introduction of *SWP* cDNA into *smp^{epi}* plants fully restored them to wild-type, but the expression of both *SMP1* and *SMP2* were also restored in these lines, suggesting a physical interaction among the three proteins and/or genes. We propose that step II splicing factors and a transcriptional Mediator-like complex are involved in the timing of cell cycle arrest during leaf development.

INTRODUCTION

Plant cells do not move and are surrounded by a rigid cell wall, and for this reason, cell division rates and patterns were thought to be directly responsible for generating new structures during development. However, despite genetic manipulation of either cell proliferation or cell expansion, the resulting organs and/or organisms often attain the normal size (Hemerly et al., 1995; Smith et al., 1996; Cleary and Smith, 1998; Jones et al., 1998; Wang et al., 2000; De Veylder et al., 2001; Autran et al., 2002). They may consist of fewer but larger cells, or more numerous but smaller cells, suggesting that cell division can be uncoupled from iterative plant development. Similarly, in animals, generally, changes in cell size can be compensated for by changes in cell number to maintain the final size of an organism, suggesting a lack of correlation between cell division and the formation of complex structures during development (reviewed in Day and Lawrence, 2000; Weinkove and Leevers, 2000). Furthermore, during the growth and development of the leaf organ primordium, for example, there are no fixed patterns of cell division, but rather a stochastic gradient of cell division arrest from the distal tip to the base of the leaf (Donnelly et al., 1999).

The accumulating evidence of cell division–independent mechanisms of development has lead to a long debate on the actual function or necessity of cell division in plant development (reviewed in Doonan, 2000). However, more recent evidence has assigned developmental significance to cell cycle progression and exit. For example, experiments using cell cycle inhibitors and in particular DNA synthesis inhibitors have shown that, unlike cytokinesis, cell cycle progression is coupled to meristem growth and patterning (Grandjean et al., 2004). Also, the overexpression of the D-type cyclin *CYCD3;1*, unlike most other cell cycle proteins, inhibited several cell differentiation pathways in the leaf, indicating an important role in leaf development (Dewitte et al., 2003). More specifically, *CYCD3;1* overexpression reduced the proportion of cells in the G_1 phase of the cell cycle, suggesting that cell cycle exit at the G_1 phase is required for proper execution of differentiation in the leaf (Dewitte et al., 2003). Similarly, in mammals, cell cycle exit has been shown to be required for skeletal myogenesis (Skapek et al., 1995; Zachsenhaus et al., 1996; Guo and Walsh, 1997) and lens fiber cell differentiation (Zhang et al., 1998). Most likely, there exists a subtle and close interplay between growth/organogenesis and cell cycle progression/exit, and this relationship is defined by developmental context.

[1] To whom correspondence should be addressed. E-mail timothy.nelson@yale.edu; fax 203-432-5711.

The author responsible for distribution of materials integral to the findings presented in this article in accordance with the policy described in the Instructions for Authors (www.plantcell.org) is: Timothy Nelson (timothy.nelson@yale.edu).

Article, publication date, and citation information can be found at www.plantcell.org/cgi/doi/10.1105/tpc.105.032771.

The relationship among D-type cyclins, G_1 phase cell cycle exit, and leaf cell differentiation is intriguing because in all eukaryotes, the G_1 phase seems to be a major checkpoint in the decision to stop or to continue cell proliferation. In plants, like in animals, the initiation of cell division probably involves the inactivation of the retinoblastoma protein by the appropriate cyclin-dependent kinases and D-cyclins. This would involve two transcription factors, E2F and Dpa, which, also in plants, are involved in the activation of the cell cycle genes and in the maintenance of meristematic competence (De Veylder et al., 2002). During cell differentiation, the opposite process is thought to occur (i.e., a reactivation of the retinoblastoma blocks the cells

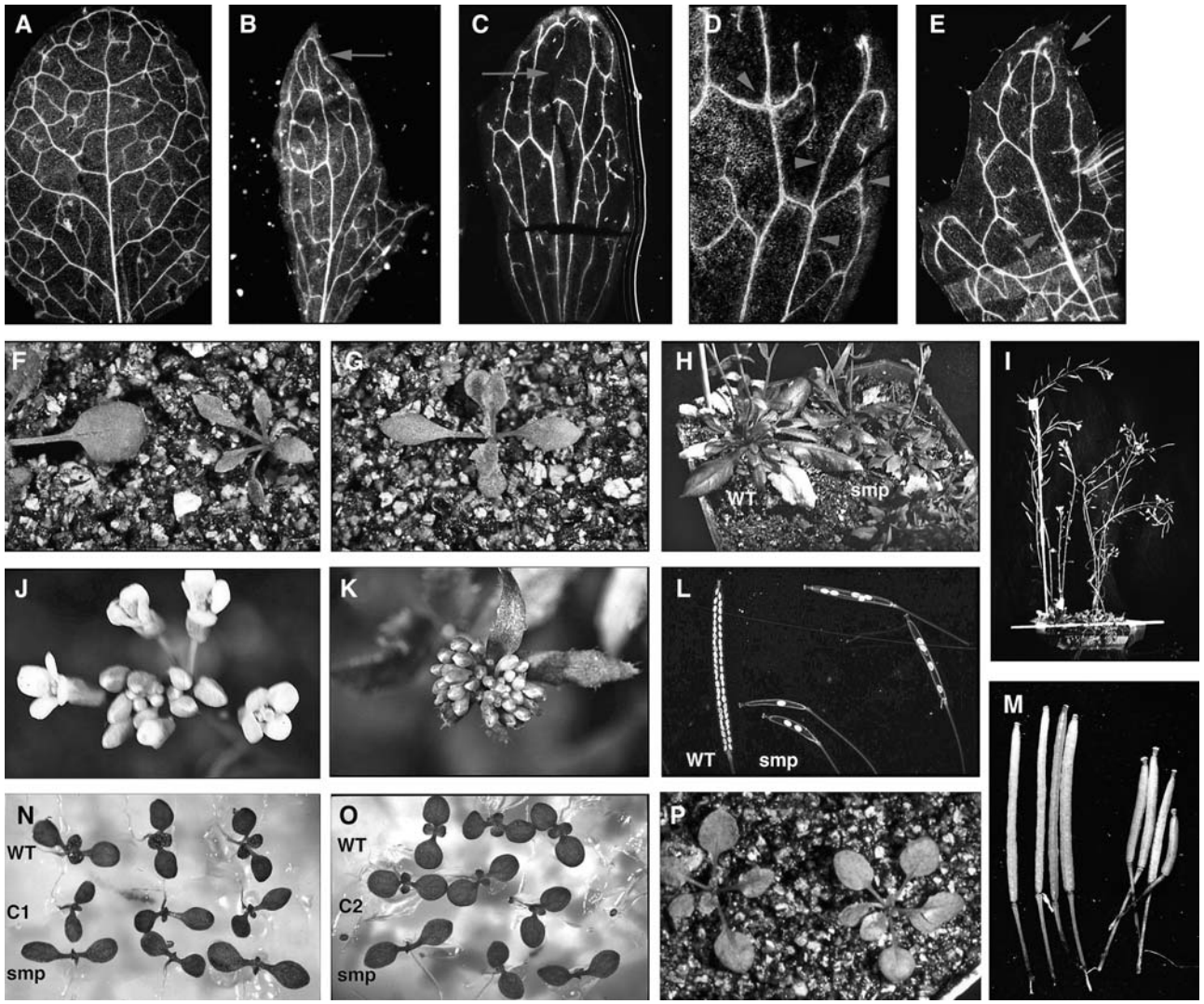

Figure 1. General Plant Phenotype of the *smp* Mutant.

(A) to **(E)** Cleared leaves viewed under dark-field illumination. The wild type is in **(A)**, and *smp* is in **(B)** to **(E)**. **(D)** is a close-up of the veins in *smp*. Arrowheads point to axialization defects in veins. Arrows point to discontinuities in the venation pattern.

(F) and **(G)** Leaf shape and size of 2-week-old plants grown on soil. The wild type (left in **[F]**) and *smp* (**[G]** and right in **[F]**).

(H) Leaf rosettes of 4-week-old wild-type (left) and several *smp* (right) plants.

(I) Fully-grown wild-type (left) and *smp* (right) plants.

(J) and **(K)** Inflorescences of the wild type **(J)** and *smp* **(K)**.

(L) and **(M)** Mature green wild-type (left) and *smp* (right) siliques were viewed under bright-field illumination **(M)** or cleared and viewed under dark-field illumination **(L)** to look at seed size and number.

(N) and **(O)** Week-old *smp* seedlings containing a transgenic copy of *SMP* gene and exhibiting a partially restored phenotype (C1) or a wild-type phenotype (C2) were grown on agar media, and the outgrowths of the first two leaves were compared with those of wild-type (top row) and untransgenic *smp* (bottom row) seedlings.

(P) Leaf shape and size of 2- to 3-week-old wild-type (left) and C1 (right) plants.

in G_1, inducing cell differentiation) (Ach et al., 1997). Much more work needs be done to uncover the players and mechanisms regulating cell proliferation in organs and/or organisms.

In a screen for leaf development mutants, we identified a recessive mutant, *swellmap* (*smp*), with reduced leaf organ size and cell number. This defect is partially compensated for by an increase in final cell size. The recessive mutation proved to be epigenetic and defined a single locus, *SMP1*, that was differently methylated but affected the expression of both *SMP1* and a second very similar gene, *SMP2*, both of which encode putative step II splicing factors, which are involved in 3′ splice site selection. Genetic knockouts demonstrate that the genes are functionally redundant and developmentally essential. *SMP1* expression is associated with regions of cell proliferation in lateral organs, and overexpression of *SMP1* similarly reduced leaf organ size but increased cell number. The smp^{epi} mutation affects the transcription of the cell proliferation gene *STRUWWELPETER* (*SWP*), whose protein has similarities to Med150/Rgr1-like subunits of the Mediator complex, which is required for transcriptional activation, suggesting that SWP is the direct target of SMP1 and/or SMP2.

RESULTS

smp Mutation Affects Cell Number and Size

A single allele of the *smp* mutant was identified from a mutant screen by a reduced amount of leaf venation and a narrow, pointed venation pattern, both of which were reflected in the leaf shape and size (Figures 1A to 1H). This phenotype was completely penetrant and affected all leaf-like organs except for cotyledons. Besides the reduction in leaf organ size (less than half that of the wild type for all rosette leaves; Figure 1F), there were pronounced serrations at the marginal teeth, and the veins themselves were not properly axialized; that is, the vein cell files were not aligned from end to end in a smooth, tight bundle and instead had spaces between them (Figure 1D). Frequently, there were discontinuities in the midvein at the leaf tip, and the polar ends of vein cells did not join near the leaf margins (Figures 1B, 1C, and 1E). The mutant phenotype was first evident at the seedling stage by the retarded outgrowth of the first pair of leaves and slightly reduced root growth (Figure 1N). Fully grown *smp* plants were reduced in stature, had narrower and/or shorter organs on the whole, and were fairly infertile, producing only a few siliques (seed-bearing pods) that contain fewer but larger seeds (Figures 1I, 1L, and 1M). Moreover, a few *smp* floral meristems produced clustered floral buds (Figure 1K), which were spaced normally later in development.

Because of their conspicuous and developmentally familiar nature, leaves were used to study the more cellular aspects of the *smp* mutation. Transverse sections through *smp* leaves revealed that the leaves were wider and that aside from vascular cells, which were normally sized, all other leaf cells were fewer in number and larger in size (Figure 2D). Cell numbers were quantified through transverse sections of three fully grown leaves from the second pair of leaves to arise from each genotype

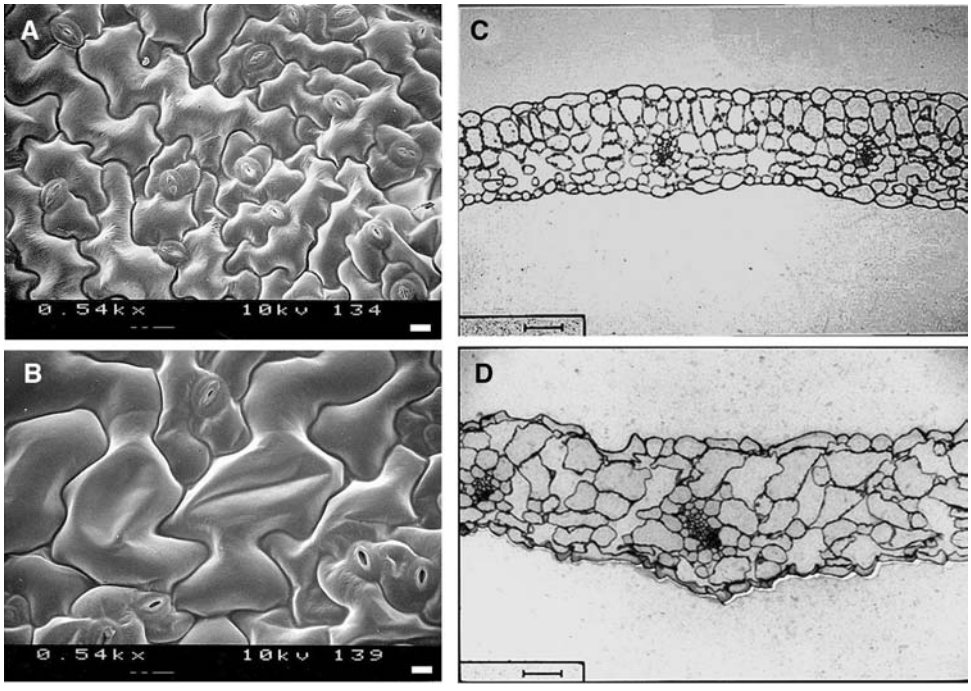

Figure 2. Leaf Cell Number and Size Are Affected in the *smp* Mutant.

(A) and **(B)** Scanning electron micrographs of the adaxial surface of fully expanded rosette leaves. **(A)** Wild-type; **(B)** *smp*. White bar on the bottom right = 10 μm.

(C) and **(D)** Transverse sections through fully expanded rosette leaves. **(C)** Wild-type; **(D)** *smp*. Bar = 50 μm.

(vascular cells were excluded), and the mean cell number in the mutant (95 cells, SD of 8.3; 0.11 mm^2) was found to be 45.2% of that in the wild type (210.2 cells, SD of 5; 0.11 mm^2). Similarly, scanning electron micrographs of *smp* leaves confirmed that the epidermal layer consisted of fewer but larger cells (Figure 2B) and that this increase in cell size was not enough to fully restore final organ size to that of the wild type. Thus, the smaller leaf size in the mutant was due to a reduction in the number of cells per leaf, and this reduction was partially compensated for by an increase in final cell size. Interestingly, although the longitudinal vascular pattern was severely reduced, the transectional vascular pattern (the arrangement of xylem and phloem) was normal except that the veins were slightly thicker.

To determine if the reduced cell number in *smp* leaves was due to a contraction of the cell proliferation phase or to a reduction in the rate of division during organ development, transverse sections of leaf primordia were taken at various time points during the cell proliferation phase of leaf development. Meristematic cells appear as small, densely stained cells in contrast with expanding vacuolated cells. Relative to the wild type, mutant leaf primordia had significantly more cells that were vacuolated and larger sized, suggesting that those cells had prematurely exited the cell proliferation phase (Figures 3D to 3F) Also, the sections revealed large intercellular spaces developing within the organ (Figures 3G to 3I), suggesting that meristematic cells were not proliferating fast enough to keep up with the expanding epidermal cell layer (i.e., a retarded rate of cell division) or that a cell wall defect led to such a schizogenous-like separation of tissues. Whatever the cause of these large intercellular spaces, their development accounts for the disorganization of the inner cell layers (particularly the palisade layer) seen later on in mature leaves (Figure 2D).

To see if *smp*'s effect on cell proliferation extended beyond leaves, we examined the structure of the inflorescence shoot apical meristem (SAM), the formation of floral organs at the meristem's periphery, and the structure of the inflorescence stem just below the youngest silique. Longitudinal sections through *smp* SAMs indicated that the organization into layers (at least for the first two layers) was not disrupted, although the layers consisted of fewer meristematic cells (Figure 9C). Floral organ formation appeared normal, albeit with reduced cell numbers (Figure 9C). The same is true for the stem (data not shown).

SMP1 and *SMP2* Encode Putative Step II Splicing Factors

A map-based cloning strategy was used to isolate the gene. Genetic analysis of F2 progeny indicated that the *smp* mutant phenotype segregated as a single recessive locus. The *smp* mutation was mapped initially between simple sequence length polymorphic markers nga111 and AthGENEA on the bottom of chromosome 1 and then finely mapped to a region on BAC F1E22 that spanned five predicted genes. Sequencing of all five genes in the mutant background did not reveal any detectable molecular lesion or point mutation. One of the genes (At1g65660) encodes a CCHC zinc finger protein that is 22% identical to the yeast SLU7 protein, a step II splicing factor involved in 3′ splice site selection (Figure 4B; Frank and Guthrie, 1992). Constitutive expression of a single locus of the wild-type transgene fully complemented the *smp* mutation in at least two independent lines (Figure 1O). Furthermore, expression of this gene by its

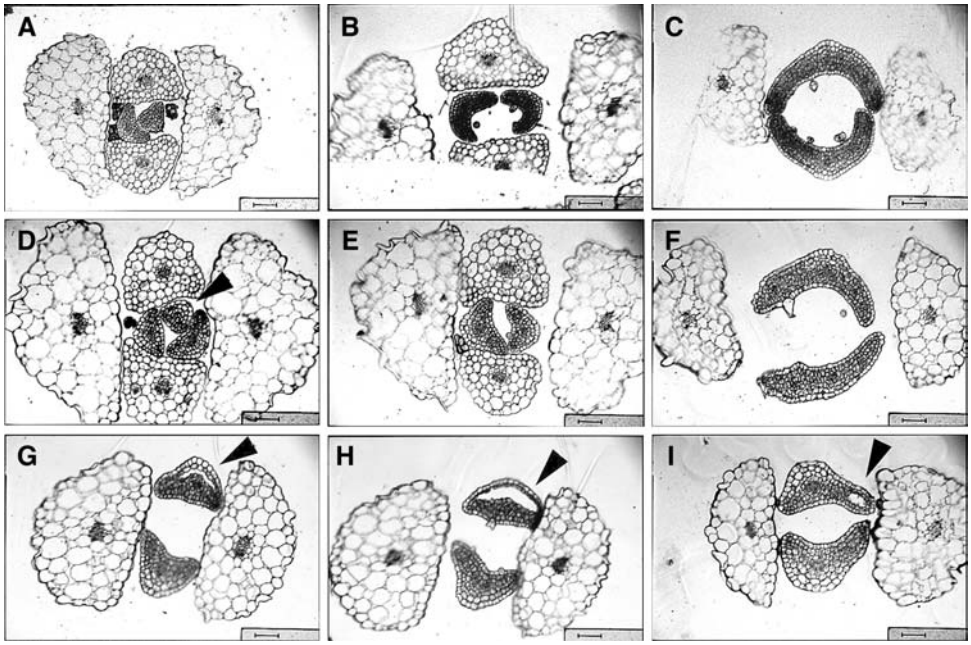

Figure 3. Precocious Arrest of Cell Proliferation in Leaf Primordia of the *smp* Mutant.

Transverse sections through leaf primordia of 7- to 9-d-old wild-type (**[A]** to **[C]**) and *smp* (**[D]** to **[I]**) seedling were arranged in developmental order from **(A)** to **(C)** and from **(D)** to **(F)**. **(G)** and **(H)** are serial sections of the same plant. Arrowheads point to large intercellular spaces. Bar = 50 μm.

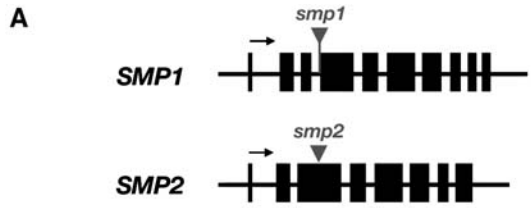

B

```
SWELLMAP   MATASV---- ---------- AF-----KSR EDHRKQIELE EARKAGLAPA EVDEDGKEIN PHIPQYMSSA PWYLN----- --SEKP---- ----------   60
AT4G37120  MATASV---- ---------- AF-----KSR EDHRKKLELE EARKAGLAPA EVDEDGKEIN PHIPEYMSKA PWYLK----- --SEQP---- ----------   60
hSLU7      MSATVVDAVN AAPLSGSKEM SLEEPKKMTR EDWRKKKELE EQRKLGNAPA EVDEEGKDIN PHIPQYISSV PWYID----- -PSKRP---- ----------   80
SLU7       MNNNS----- ---------- --------RN NENRSTIN-R NKRQL----Q QAKEKNENI- -HIPRYIRNQ PWYYKDTPKE QEGKKPGNDD TSTAEGGEKS   70

SWELLMAP   -SLKHQR-KW KSDPNY---- ---------- TKSWYDRGAK -IFQAEKYRK GACQNCGAMT HTAKACMDRP RKIGAKYTNM NIAPDE--KI ES-FELDYDG  140
AT4G37120  -SLKHQK-NW KIEPEP---- ---------- KKIWYDRGKK -IYQAEQYRK GACINCGAMT HSSKACMDRP RKIGAKYTNM NIAADE--KI ES-FELDYDG  140
hSLU7      -TLKHQRPQP EKQKQF---- --------SS SGEWYKRGVK ENSIITKYRK GACENCGAMT HKKKDCFERP RRVGAKFTGT NIAPDE--HV QPQLMFDYDG  165
SLU7       DYLVHHRQKA KGGALDIDNN SEPKIGMGIK DEFKLIRPQK -MSVRDSHSL SFCRNCGEAG HKEKDCMEKP RKMQKLVPDL NSQKNNGTVL VRATDDDWDS  169

SWELLMAP   KRDRWNGYDP STYHRVIDLY EAKEDARKKY LKEQQLKKLE EKNNNEKGDD ANSDGEEDED DLRVDEAKVD E-SRQMDFAK VEKRVRTTGG GSTG----TV  235
AT4G37120  KRDRWNGYDT STYRHVVDRY DAKEEARKKY LKEQQLKKLE EKNNNENGDD ATSDGEEDLD DLRVDEAKVD E-SRQMDFAK VEKRVRTTGG GSTG----TV  235
hSLU7      KRDRWNGYNP EEHMKIVEEY AKVDLA-KRT LKAQ--KLQE ELASGKLVEQ ANSPKHQWGE EEPNSQMEKD HNSEDEDEDK YADDIDMPGQ NFDSKRRITV  262
SLU7       RKDRWYGYSG KEYNELISKW ERDK--RNK- IKGKDKS--- ---------- ---------- QTDETLWDTD EEIELMKLEL YKDSVGSLKK DDADNSQLYR  243

SWELLMAP   RNLRIREDTA KYLLNLDVNS AHYDPKTRSM REDPLPDADP NDK-F-YLGD NQYRNSGQAL EFKQLNIHSW EAFDKGQDMH MQAAPSQAEL LYKSFQVAKE  333
AT4G37120  RNLRIREDTA KYLLNLDVNS AHYDPKTRSM REDPLPDADP NEK-F-YLGD NQYRNSGQAL EFKQINIHSC EAFDKGHDMH MQAAPSQAEL LYKNFKVAKE  333
hSLU7      RNLRIREDIA KYLRNLDPNS AYYDPKTRAM RENPYANAGK NPDEVSYAGD NFVRYTGDTI SMAQTQLFAW EAYDKGSEVH LQADPTKLEL LYKSFKVKKE  362
SLU7       TSTRLREDKA AYLNDINSTE SNYDPKSRLY KTETLGAVDE KSKMF----- ---------- ---------- ---------- ---------- ----------  288

SWELLMAP   KLKSQTKDTI MDKYGNAATE DEIPMELLLG QSERQVEYDR AGRIIKGQEV ILPKSKYEED VHANNHTSVW GSYWKDHQWG YKCCQQIIRN SYCTGSAGIE  433
AT4G37120  KLKTQTKDTI MEKYGNAATE GEIPMELLLG QSERQIEYDR AGRIMKGQEV IIPKSKYEED VHANNHTSVW GSWWKDHQWG YKCCQQTIRN SYCTGSAGIE  433
hSLU7      DFKEQQKESI LEKYGGQEHL DAPPAELLLA QTEDYVEYSR HGTVIKGQER AVACSKYEED VKIHNHTHIW GSYWKEGRWG YKCCHSFFKY SYCTGEAGKE  462
SLU7       ---------- ---------- ---------- ---------- ---------- ---------- ---------- ---------- ---------- ----------  288

SWELLMAP   AAEAALDLMK ANIARKEATE ESPKKV---- ---------- --------EE KRMASWGTDI PEDLELNEEA LANALKKEDL SRREEK--DE RKRKYNVKY-  508
AT4G37120  AAEASIDLMK ANIARKEASK ESPKKV---- ---------- --------EE KKMATWGTDI PEDLELNEEA LANALKKEDL SRREEK--DE RKRKYNVNY-  508
hSLU7      IVNSEECIIN -----EITGE ESVKKPQTLM ELHQEKLKEE KKKKKKKKKK HRKSSSDSDD EEKKHEKLKK ALNAEEARLL HVKETMQIDE RKRPYNSMYE  557
SLU7       ---------- -------RRH LTGEGLKLNE LNQFARSHAK EMGIRDEIED KEKVQHVLVA NPTKYEYLKK KREQEETKQP KIVS-IGDLE ARK-------  363

SWELLMAP   NNDVT--PEE MEAYRMKRVH HEDPMKDFL- ---------- ----------          535
AT4G37120  TNDVT--SEE MEAYRMKRVH HEDPMRNFPG ---------- ----------          536
hSLU7      TREPT--EEE MEAYRMKRQR PDDPMASFLG Q--------- ----------          586
SLU7       -VDGTKQSEE QRNH------ ----LKDLYG ---------- ----------          382
```

Figure 4. *SMP1* Encodes a Putative Step II Splicing Factor.

(A) Genomic structure of the *SMP1* and *SMP2* genes. Black boxes indicate exons. Arrows indicate direction of transcription. SALK T-DNA insertions are indicated for the *smp1* and *smp2* insertion alleles.

(B) Alignment of the deduced amino acid sequences of SMP1, AT4G37120 (SMP2), yeast SLU7 (Frank and Guthrie, 1992), and human hSLU7 (Chua and Reed, 1999). The CCHC domain is underlined. Shared amino acids are shaded.

native promoter (810 bp of upstream sequence) gave partial rescue during the first week of growth and then a full rescue hereafter (Figures 1N and 1P). The constitutive expression of a C-terminal translational fusion of the putative *SMP* gene to *smGFP* (*SMP*:*GFP*) also fully rescued the mutant in at least two independent lines. Thus, At1g65660 was identified as the *SMP* gene and is very similar to another unlinked gene, At4g37120 (Figure 4B; 90% identity on an amino acid level). Hereafter, we will refer to At1g65660 and At4g37120 as *SMP1* and *SMP2*, respectively.

There was a discrepancy between the sequence of the full-length *SMP1* cDNA in GenBank (accession number BT002797) and the genomic sequence of the predicted *SMP1* coding region in that the cDNA sequence in BT002797 contained an additional exon further upstream of the predicted start codon and a single base pair change in the fourth exon. To confirm that the sequence in BT002797 is correct, *SMP1* cDNA was independently isolated from wild-type RNA, and its sequence matched that in BT002797. Thus, *SMP1* coding sequence consists of 10 exons that span a 2.6-kb genomic region (Figure 4A).

The CCHC zinc finger motif ($CX_2CX_4HX_4C$), also known as retroviral-type zinc finger, is found in the nucleocapsid proteins of RNA retroviruses (e.g., Moloney murine leukemia virus [Shinnick et al., 1981], Rous sarcoma virus [Schwartz et al., 1983], and human immunodeficiency virus [Wain-Hobson et al., 1985]); in transposable elements (e.g., Drosophila Copia [Mount and Rubin, 1985] and yeast Ty element 3-2 [Hansen et al., 1988]); and in developmental proteins (e.g., Drosophila Nanos [Curtis et al., 1997], human CNBP [Rajavashisth et al., 1989], and *Caenorhabditis elegans* glH-1 [Roussell and Bennett, 1993]). All of the above have been demonstrated to bind to single-stranded nucleic acids. Based on the sequence similarity to the yeast step II splicing factor SLU7 outside the zinc finger motif, SMP1 and SMP2 most likely bind RNA (Figure 4B). SMP1 and SMP2 contain no other recognizable motif or targeting signal peptide.

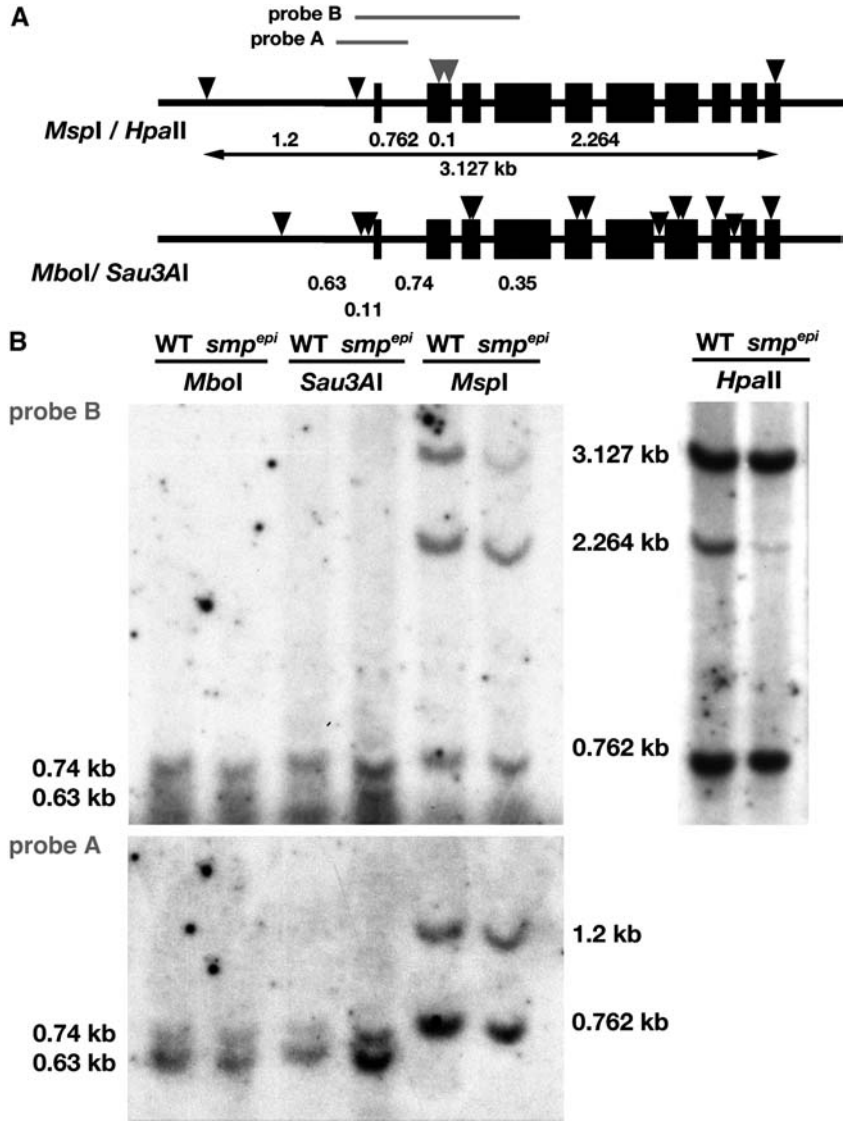

Figure 5. *SMP1* Is Hypomethylated in *smp*^{epi}.

(A) Restriction maps of the *SMP1* locus. Black boxes indicate exons, and arrowheads indicate recognition sites recognized by methylation-insensitive restriction enzyme *Mbo*I and methylation-sensitive enzymes *Bgl*II, *Hae*III, *Nco*I, *Sau3*AI, *Hpa*II, and *Msp*I. Gray arrowheads indicate sites found to be methylated.

(B) DNA gel blots of digested DNA from wild-type and homozygous *smp*^{epi} plants were hybridized with either ^{32}P-labeled probe A (bottom) or ^{32}P-labeled probe B (top). Note the presence and abundance of 3.127-kb band in the *Msp*I digest of wild-type DNA, the reduction of 3.127-kb band in the *Msp*I digest of *smp*^{epi}, and the reduction of 2.265-kb band in *Hpa*II digest of *smp*^{epi}.

Epigenetic Mutation Defines One Locus but Affects the Expression of Two Loci

No molecular lesions or base pair changes were found in the coding and upstream sequences of the *SMP1* gene in the *smp* mutant, leading us to explore epigenetic changes in the region. Epigenetic phenomena in general exhibit genetic instability. For example, the *clark kent-3* epigenetic allele of *SUPERMAN* exhibits a reversion rate of 17/586 (2.9%; Jacobsen and Meyerowitz, 1997). Similarly, *smp* has a spontaneous reversion rate of 4/151 (2.6%). Two of the four wild-type-looking plants were complete revertants; their selfed progeny segregated 3:1 wild type to mutant phenotype (10/36 = 27.8% and 8/33 = 24.2%). The partial revertants had segregation rates of 12/28 (43%) and 7/17 (41%).

To determine if the *smp* allele was generated by an epimutation, DNA methylation-sensitive restriction analysis was performed on wild-type and mutant DNA, and the digested DNA was probed with gene-specific probes to determine the overall methylation profile of the *SMP1* locus in the whole plant.

Restriction endonucleases *Hpa*II and *Msp*I recognize the same sequence, CCGG, but differ in their sensitivity to methylation. *Msp*I will not cut if the outer cytosine is methylated, and *Hpa*II will not cut if either of the two cytosines is methylated. When the DNA gel blots were probed with a promoter fragment (Figure 5A; probe A), bands of expected size appeared, suggesting that those sites in the promoter were unmethylated and that the digests were complete. When the DNA gel blots were probed with a coding fragment (Figure 5A; probe B), bands larger than expected were found in both the digests, suggesting that cytosine methylation existed at two CCGG sites in the coding sequence, more specifically, the 2nd exon (Figure 5B). The presence and abundance of a 3.127-kb band in the *Msp*I digest of wild-type DNA and the reduction of the same band in the *Msp*I digest of *smp*^{epi} DNA indicated that the outer cytosines at both CCGG sites were hypomethylated in the mutant. Conversely, the reduction of a 2.265-kb band in *Hpa*II digest of *smp*^{epi} compared with that of the wild type indicated that the inner cytosines were hypermethylated in the mutant. Together, the DNA gel blots suggest that (1) both cytosines of CCGG sites in the 2nd exon of *SMP1* gene are heavily methylated in the wild type and that (2) those cytosines are differently methylated in mutant plants. Methylation was not detected in either the wild type or mutant allele using methylation-sensitive restriction endonucleases *Bgl*II, *Bst*B1, *Cla*I, *Hae*III, *Nco*I, *Pst*I, *Pvu*I, *Pvu*II, and *Sau3*AI (Figures 5A and 5B; data not shown), suggesting that the methylation pattern at CCGG sites in the 2nd exon may be responsible for the mutant phenotype. Because the mutant allele was most likely generated by an epimutation, it was renamed *smp1*^{epi}.

Two additional alleles (*smp1-1* and *smp2-1*) were identified that contain a T-DNA insertion in the third intron of the *SMP1* gene and third exon of the *SMP2* gene, respectively (Figure 6A; Alonso et al., 2003). RT-PCR results confirmed that *SMP1* and *SMP2* transcripts were undetectable in *smp1-1* and *smp2-1* homozygous plants, respectively (Figure 6B), indicating that both alleles are null. Surprisingly, plants homozygous for either insertion allele looked wild-type (Figure 7A), suggesting that the genes have redundant functions and similar or overlapping expression patterns. Furthermore, RT-PCR results indicated that the transcripts of both *SMP1* and *SMP2* were reduced in *smp1*^{epi} homozygous plants (Figure 6B), suggesting that the *smp1*^{epi} mutation induced transcriptional silencing of both *SMP1* and *SMP2* genes.

To recapitulate the *smp*^{epi} mutant phenotype, we crossed homozygous *smp1-1* plants to homozygous *smp2-1* plants, identified wild-type-looking F2 plants that were homozygous for one mutation and heterozygous for the other, allowed them to self-pollinate, grew the F3 on agar plates, and looked for double mutants that should make up one-quarter of the population. All F3 plants looked wild-type, and PCR genotyping of individual plants indicated that although both mutations segregated normally in the F2 population ($n = 40$), no F3 was found to be

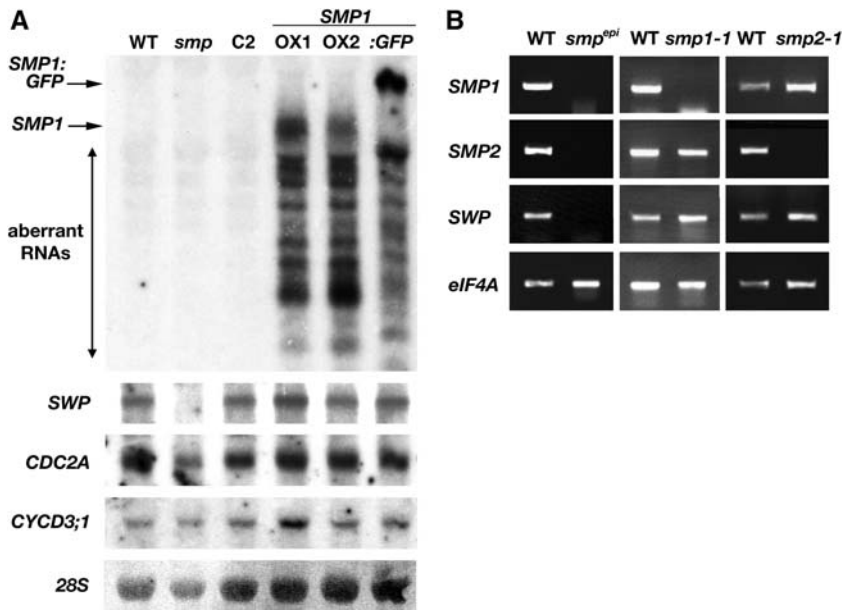

Figure 6. *SMP1* mRNA Expression Analyses.

(A) RNA gel blot with 10 μg of total RNA was hybridized with a ^{32}P-labeled *SMP1* probe corresponding to the second exon of the cDNA, *SWP* probe corresponding to the 3′ end of the cDNA, *CDC2A* probe, or *CYCD3;1* probe. Methylene blue–stained *28S* RNA was the loading control. C2 refers to an *smp*^{epi} plant that contained a transgenic copy of the *SMP1* gene and exhibited a wild-type phenotype. OX1 and OX2 refer to independent *SMP1*-overexpressing lines. SMP1:GFP refers to a wild-type plant that contains a transgenic copy of a C-terminal translational fusion of the *SMP1* gene to the *smGFP* gene.

(B) Total RNA from wild-type, *smp*^{epi}, *smp1-1*, and *smp2-1* plants was reverse transcribed and PCR amplified using primers to *SMP1*, *SMP2*, and *SWP* cDNAs, and where applicable, to a region upstream of the SALK T-DNA insertion site. RT-PCR products were run on an ethidium bromide–stained gel. PCR-amplified *eIF4A* was the loading control.

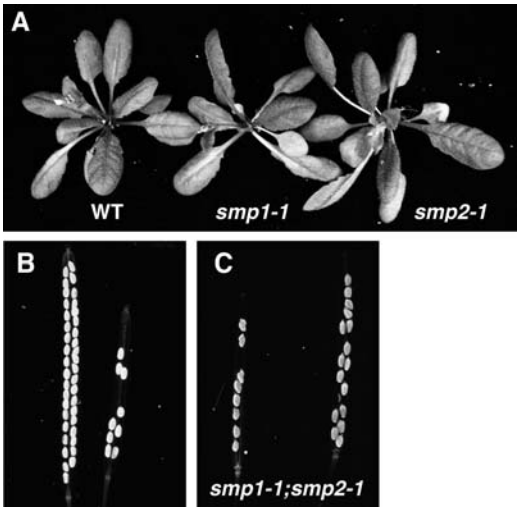

Figure 7. *SMP1* and *SMP2* Are Functionally Redundant and Essential.

(A) Wild-type, *smp1-1*, and *smp2-1* plants, respectively.
(B) and **(C)** Siliques (seed-bearing pods) taken from plants homozygous for *smp1-1* and heterozygous for *smp2-1* were cleared and viewed under dark-field illumination. The silique on the left in **(B)** is wild-type and was used for comparison.

homozygous for both mutations ($n = 39$), suggesting that the double mutant was not viable. We examined the siliques taken from F2 plants and found that approximately one-quarter to one-half of the seeds were missing (Figures 7B and 7C), suggesting that the double mutant was not viable at the gametophytic and/or embryo stage. Because reduced expression of *SMP1* and *SMP2* in the *smp^{epi}* mutant resulted in fertility defects, the observed lethality of the double mutant further indicated that the functionally redundant genes are essential.

SMP1 Expression Is Associated with Regions of Cell Proliferation in Lateral Organs

The expression pattern of *SMP1* was visualized by RNA in situ hybridizations as well as histochemical staining of plants containing a transgenic copy of the *SMP1* promoter driving the β-*glucuronidase* (*GUS*) reporter gene. *SMP1* mRNA expression was found throughout early globular-staged embryos (Figure 8A), and expression intensified in the cotyledon primordia of heart-staged embryos (Figure 8B). The broad expression pattern persisted through embryogenesis (Figures 8G and 8H) until the bent cotyledon stage where *SMP1* promoter activity increased in procambial cells (Figure 8I). After germination, *SMP1* mRNA expression was found throughout leaf primordia but not in the SAM (Figure 8C). *SMP1* promoter activity was also found throughout very young leaf primordia (Figure 8J) and as the leaf matured, was turned off in a tip-to-base manner (Figure 8K). This pattern of GUS expression overlapped with the general pattern of cell proliferation and presaged the basipetal wave of cell maturation that would flow from leaf tip to leaf base. This pattern of GUS expression also holds true for lateral root primordia (Figure 8L). In general, *SMP1* expression is associated with regions of cell proliferation in lateral organs.

Overexpression of SMP1 Affects Cell Number and Size

To look at SMP1 function, we overexpressed the *SMP1* gene using the constitutive 35S promoter of Cauliflower mosaic virus (*35S CaMV*). We characterized five lines that contained either the *35S CaMVp*:*SMP1* or *35S CaMVp*:*SMP1*:*smGFP* construct and gave a similar dominant heritable phenotype. *SMP1* transcript levels in three of those lines were examined, and the observed phenotype was associated with an overproduction of *SMP1* mRNA of the expected size (Figure 6A; ~2 kb). In *SMP1*:*GFP* plants, a single band of ~2.7 kb was observed, consistent with the expected size of the mRNA (Figure 6A). Many smaller discrete bands were also detected, suggesting posttranscriptional silencing of that transcript.

Overall, *SMP1* overexpression reduced leaf organ size and stem internodal length. All five *SMP1*-overexpressing lines generated plants exhibiting clustered siliques (Figure 9B), which were slightly crinkled and contained fewer but larger seeds (data not shown). Three of those lines also produced a few plants that were phenotypically more severe and resembled severe dwarfs. More specifically, their inflorescences were very reduced in stature and produced smaller cauline leaves (Figure 9C).

Because a similar reduction in leaf organ size was observed for both *SMP1*-overexpressing plants and *smp^{epi}* mutant plants, histological analyses were used to compare their cell size and number relative to that of the wild type. Sections through cauline leaves of phenotypically severe *SMP1*-overexpressing plants indicated that the leaves were thinner and their cells were more numerous but smaller per area than those observed in the wild type (Figures 10B and 10E). Cell numbers were quantified through transverse sections of three fully grown cauline leaves from each genotype (vascular cells were excluded), and the mean cell number in *SMP1*-overexpressing leaves (220.3 cells, SD of 11.9; 0.11 mm^2) was found to be 110.2% of that in the wild type (200 cells, SD of 1.2; 0.11 mm^2). Inflorescence shoot apices were also examined, and scanning electron micrographs of the epidermal layer of the third or fourth stem internode from the youngest silique indicated that *SMP1* overexpression interfered with cell elongation. The overall pattern of cell expansion was complex, but a few interspersed cells were shorter and wider (Figure 9E).

Regulatory Role in Expression of the Cell Proliferation Gene *SWP*

Several characterized *Arabidopsis thaliana* genes are thought to play a role in cell proliferation in lateral organs. The *SWP* gene, for example, is involved in defining the duration of the cell proliferation phase in the leaf primordium without affecting cell division rates (Autran et al., 2002). The loss-of-function and gain-of-function phenotypes of *SWP* resemble those of *SMP1* and/or *SMP2*; that is, they have similar effects on leaf organ size as well as leaf cell number and cell size. However, they have different leaf morphologies (i.e., the extent of leaf serration), which may be due to differences in ecotypic background. More importantly,

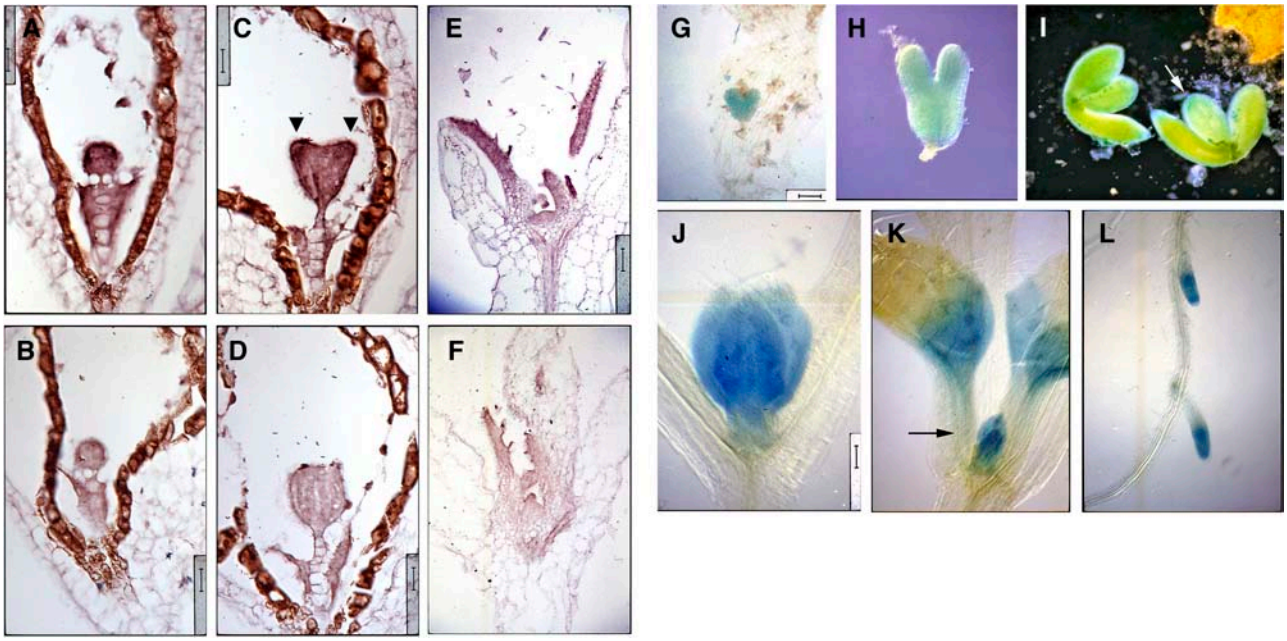

Figure 8. *SMP1* Expression Is Associated with Regions of Cell Proliferation.

(A) to **(F)** Longitudinal sections were hybridized with antisense (**[A]**, **[C]**, and **[E]**) or sense (**[B]**, **[D]**, and **[F]**) dioxigenin-labeled *SMP1* RNA probe.
(A) and **(B)** Globular-staged embryos. Bar = 16 μm.
(C) and **(D)** Heart-staged embryos. Arrowheads point to cotyledon primordia. Bar = 16 μm.
(E) and **(F)** Developing leaves and leaf primordia of week-old seedlings. Bar = 50 μm.
(G) to **(L)** Wild-type plants containing a transgenic copy of the *SMP* promoter-driven *GUS* reporter gene were stained for GUS activity and viewed under bright-field illumination unless noted otherwise.
(G) Heart-staged embryo. Bar = 50 μm.
(H) Torpedo-staged embryo. Bar = 31.25 μm.
(I) Bent cotyledon-staged embryos viewed under dark-field illumination because of saturated GUS staining under bright-field illumination. Arrow points to stronger GUS staining in the procambial strands of the cotyledons. Bar = 100 μm.
(J) Developing leaves of a 7-d-old seedling. Bar = 66 μm.
(K) Developing leaves and leaf primordia of a 9-d-old seedling. Arrow points to GUS-stained leaf primordia. Bar = 100 μm.
(L) GUS-stained lateral root primordia of a week-old seedling. Bar = 100 μm.

unlike *smp*^{epi}, the *swp* mutation affects the maintenance of the SAM. The *SWP* gene encodes a protein with similarities to Med150/Rgr1-like subunits of the Mediator complex, which is required for RNA polymerase II recruitment at target promoters in response to specific transcriptional activators. Given the strong phenotypic similarities between *smp*^{epi} and *swp* plants and their effects on the duration of the cell proliferation phase, *SWP* expression level was examined by RNA gel blot analysis and RT-PCR and was found to be undetectable in *smp*^{epi} plants but normal in *SMP1*-overexpressing plants and in *smp1-1* and *smp2-1* insertion lines (Figures 6A and 6B), suggesting that *SWP* transcription depends on the expression of *SMP1* and/or *SMP2* and that the reduction of *SWP* transcription is responsible for much of the *smp*^{epi} phenotype.

To demonstrate that the primary regulatory role for both putative step II splicing factors, SMP1 and SMP2, is in the transcription of *SWP*, a construct containing the full-length *SWP* cDNA driven by the *35S CaMV* promoter was introduced into *smp*^{epi} mutant plants. Because of the moderate infertility of these plants, only four independent lines were obtained, three of which exhibited a wild-type phenotype (Figure 11A). RT-PCR results confirmed that two of these restored lines expressed a wild-type level of fully spliced *SWP* transcript and more so than the line that exhibited the mutant phenotype (Figures 11B and 11C). Surprisingly, transcript levels of *SMP1* and *SMP2* were also increased in all three lines (Figure 11B). It is highly unlikely that all three lines are complete revertants of the *smp*^{epi} mutation (reversion rate is only 2.6%), and given SWP's putative role in transcriptional activation, it is more likely that the concomitant increase of all three transcripts by the introduction of the *SWP* cDNA suggests a physical interaction among their proteins and/or genes as well as a connection between their methylation status and transcriptional status.

Interestingly, we found two CCGG sites in the 5th and 6th exons of the *SWP* gene that were highly methylated in both wild-type and *smp*^{epi} plants (Figure 12). Methylation was not detected in either the wild-type or *smp*^{epi} allele using methylation-sensitive restriction endonucleases *Bgl*II, *Bst*B1, *Cla*I, *Hae*III, *Nco*I, *Pst*I, *Pvu*I, *Pvu*II, and *Sau3*AI (Figure 12B; data not shown). Furthermore, similar to the methylation pattern found in the *SMP1* gene,

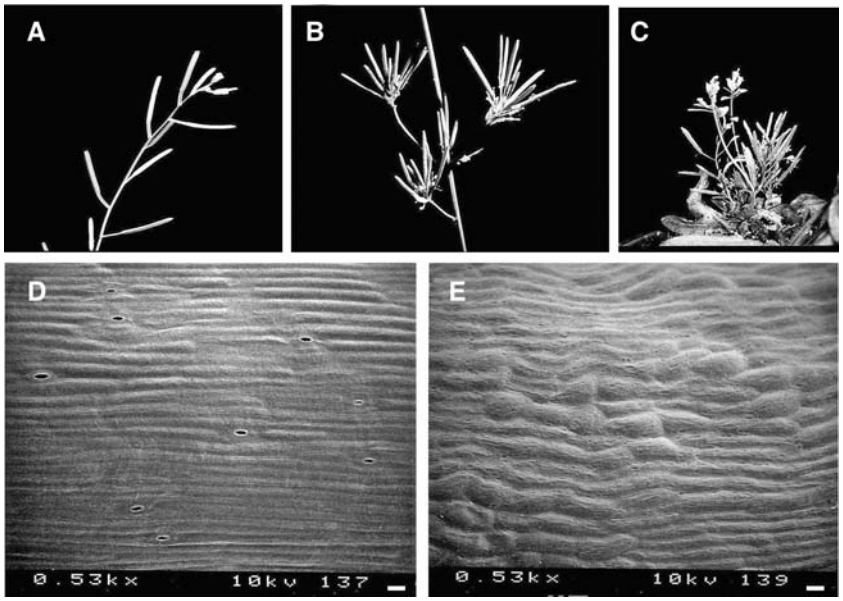

Figure 9. Internodal Cell Elongation Affected in *SMP1*-Overexpressing Lines.

(A) to **(C)** Shoot architecture. **(A)** Wild-type; **(B)** and **(C)** *SMP1*-overexpressing lines.
(D) and **(E)** Scanning electron micrographs of the third or fourth stem internode from the youngest silique. **(D)** Wild-type; **(E)** *SMP1*-overexpressing line.
White bar at the bottom right = 10 μm.

the outer and inner cytosines at those sites in the *SWP* gene were differently methylated in the mutant (Figure 12B).

Another well-characterized Arabidopsis gene involved in defining the duration of the cell proliferation phase in the leaf primordium is *AINTEGUMENTA* (*ANT*). Inactivation and overexpression of this transcription factor reduced and increased the final cell number in lateral organs, respectively, without affecting cell division rates (Mizukami and Fischer, 2000). However, there was no compensatory decrease in cell size in *ANT* overexpression plants; instead, final organ size was increased. Furthermore, *ANT* overexpression activated ectopic expression of *CYCD3;1*, which encodes a D-cyclin important for the initiation of cell division at the G_1 phase in leaves (Mizukami and Fischer, 2000). *ANT* and *CYCD3;1* expressions were examined by RNA gel blot analysis and were found to be unchanged in *smp*^{epi} and *SMP1*-overexpressing plants (Figure 6A; data not shown), suggesting that the role of *SMP1* and *SMP2* in cell proliferation regulation in leaves does not involve *ANT* nor *CYCD3;1* at the RNA level.

Aside from D-cyclins, the other major regulators of eukaryotic cell cycle initiation are cyclin-dependent kinases. In Arabidopsis, the *CDC2A* gene encodes a functional cyclin-dependent kinase homolog that is expressed in all plant meristems (Martinez et al., 1992; Hemerly et al., 1993) and, when inactivated, reduces cell proliferation in leaves while increasing cell size (Hemerly et al., 1995). *CDC2A* expression also was found to be unchanged in *smp*^{epi} and *SMP1*-overexpressing plants (Figure 6A), suggesting that at least at the RNA level, *SMP1* and/or *SMP2* acts downstream of *CYCD3;1* and *CDC2A* in cell proliferation regulation.

DISCUSSION

The recessive *smp*^{epi} allele defines a single locus because the introduction of wild-type *SMP1* genomic DNA fully rescued *smp*^{epi} homozygous plants. Also, *smp*^{epi} is a loss-of-function allele because the transcript level of *SMP1* (and *SMP2*) is reduced. Several lines of evidence indicate that the *smp*^{epi} allele is an epi-allele; it is recessive, exhibits genetic instability, is associated with a different methylation pattern of two sites in the 2nd exon of the *SMP1* gene, affects the transcription of its sister gene, and resembles a weaker version of the *smp1 smp2* double mutant. *SMP1* is one of a few Arabidopsis genes known to be methylated in the wild-type condition. Typically, methylation is positively correlated with transcriptional gene silencing, but there are notable exceptions in plants and animals. For example, in the case of the maize (*Zea mays*) paramutagenic *B′* and paramutable *B-1* alleles, the high-expressing *B-1* allele is methylated more than the low-expressing *B′* allele (Stam et al., 2002). In mouse, the maternal-specific methylation of the imprinted *Igf2r* gene is necessary for expression (Stöger et al., 1993). In the case of *smp*^{epi}, the methylation pattern is more complex.

Transcriptional gene silencing is typically associated with promoter methylation; however, we have found no methylation differences at multiple sites in the promoter. Interestingly, in the case of *SMP1*-overexpressing lines, *SMP1* transcripts appeared to undergo posttranscriptional gene silencing, which is typically associated with methylation of the coding sequence.

It would appear that the methylation status of certain cytosines in the *SMP1* gene is responsible for transcriptional silencing of not only the *SMP1* gene but also the unlinked *SMP2* gene. If that

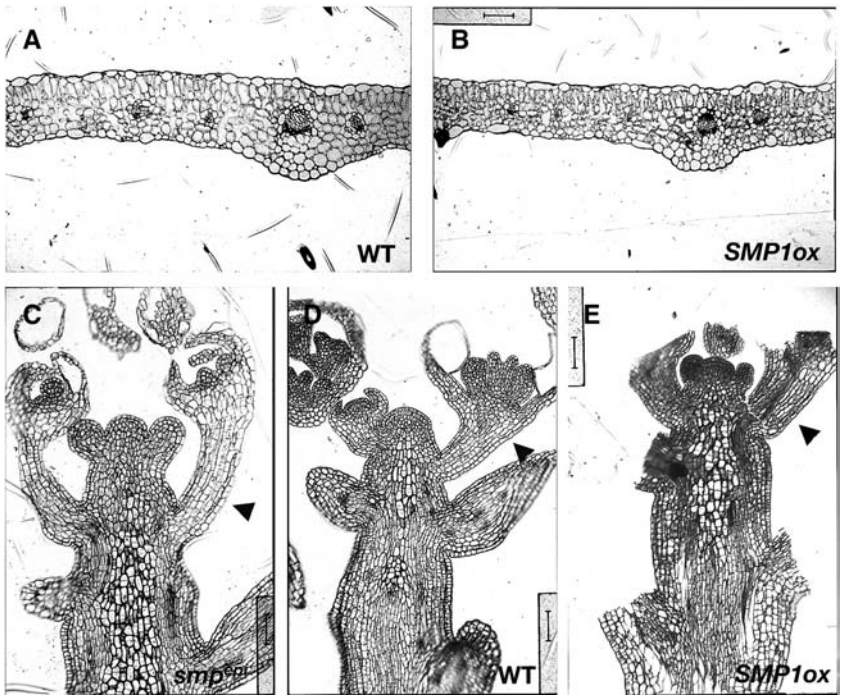

Figure 10. Overexpression of *SMP1* Affects Cell Number and Size.

(A) and **(B)** Transverse sections through fully expanded wild-type **(A)** and *SMP1*-overexpressing **(B)** cauline leaves. Bar = 62.5 μm.
(C) to **(E)** Longitudinal sections through the primary inflorescence shoot apices of *smp*^{epi} **(C)**, wild-type **(D)**, and *SMP1*-overexpressing **(E)** plants. Arrowheads point to the pedicel of a developing flower. Bar = 50 μm.

is the case, then it resembles other *trans*-silencing phenomena, which usually involve the presence of repeats as a trigger mechanism. For example, in Arabidopsis, the inverted repeat of one *pai* locus was shown to trigger methylation of all other *pai* homologs (Luff et al., 1999). Also, in maize, the tandem direct repeats in the promoter of the paramutagenic *B′* allele was shown to trigger methylation of the paramutable *B-1* allele (Stam et al., 2002). However, there are no detectable repeat structures in the promoter and coding sequences of both *SMP1* and *SMP2* genes, so it remains unclear how the methylation pattern of at least two sites in the *SMP1* gene was able to affect expression of the unlinked *SMP2* gene. Also, there are no known transposons in the vicinity of *SMP1* that can trigger epigenetic modifications, so it remains unclear how epi-alleles in general and the *smp*^{epi} allele in particular are generated. Finally, further mystery surrounds the similar methylation patterns found at CCGG sites in the coding regions of the *SMP1* and *SWP* genes because no sequence similarities were found between the two genes in the vicinity of the CCGG sites.

SMP1 and *SMP2* encode a CCHC zinc finger protein with similarities to step II splicing factors. Step II splicing factors are responsible for the selection of correct 3′ splice sites, and some had been characterized in other systems to be nonessential and play a role in the efficient progression through cell cycle transitions (e.g., Cdc40p; Vaisman et al., 1995; Boger-Nadjar et al., 1998). In fact in yeast, many splicing factors were defined by mutations that had been uncovered in cell cycle mutant screens (e.g., Prp3p, Prp8p, Prp22p, and Cef1p; Shea et al., 1994; Hwang and Murray, 1997; McDonald et al., 1999). Some splicing factors have been found to be specific for certain cellular RNAs (e.g., Prp17p on *TUB1* and *TUB3* intron splicing; Chawla et al., 2003). Because of the localization of *SMP1* mRNA expression to regions of cell proliferation in lateral organs and of the *smp*^{epi} mutation's effect on the duration of the cell proliferation phase there, most likely SMP1 and SMP2 affect the correct 3′ splicing of certain target pre-mRNA transcripts that direct cell proliferation in lateral organs. One of the functional targets of SMP1 and SMP2 is the transcription of *SWP*, and it may be the primary target because transgenic expression of a fully spliced *SWP* cDNA fully restored the *smp*^{epi} mutant to wild-type. That it also caused a concomitant increase in the expression of *SMP1* and *SMP2* suggests some interaction among the three proteins and/or genes in transcriptional activation and methylation status. Finally, the loss of function of both SMP1 and SMP2 do not adversely affect the transcription and transcript processing of cell cycle regulators *CYCD3;1* and *CDC2A*, which had been shown to be involved in cell cycle progression in leaves.

Because plant growth and organ formation do not involve cell migration or for the most part cell death, the final organ cell number mostly depends on two factors: (1) the number of cells initially recruited to the organ primordium from the meristem and (2) the proliferation of the meristematic cells in the developing organ. Cell proliferation itself can be regulated at two levels: (1) the duration of the cell proliferation phase and (2) the rate of cell

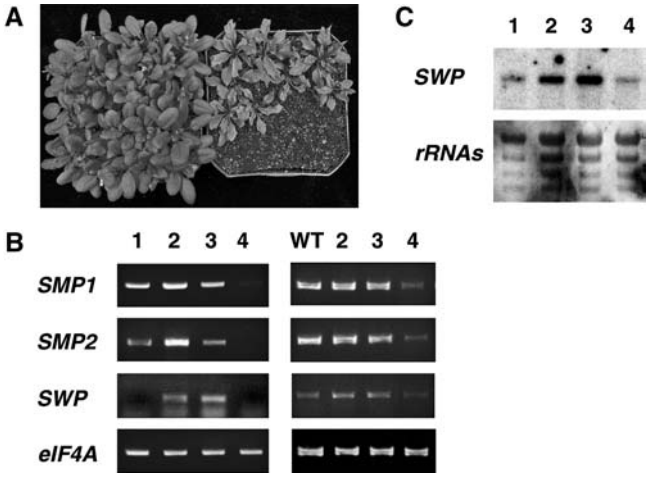

Figure 11. Genetic Interaction between *SMP1*, *SMP2*, and *SWP*.

(A) *smp*^{epi} plants containing a transgenic copy of *SWP* cDNA and exhibiting a wild-type phenotype (left; shown is line 3) or *smp*^{epi} mutant phenotype (right; shown is line 4).

(B) Total RNA from wild-type, *smp*^{epi}, and four independent *smp*^{epi} lines containing a transgenic copy of *SWP* cDNA were reverse transcribed and PCR amplified using primers to *SMP1*, *SMP2*, and *SWP*. RT-PCR products were run on an ethidium bromide–stained gel. PCR-amplified *eIF4A* was the loading control. 1, 2, and 3 refer to lines that exhibit a wild-type phenotype, and 4 refers to a line that exhibits *smp*^{epi} phenotype.

(C) RNA gel blot with 10 μg of total RNA was hybridized with a ^{32}P-labeled *SWP* probe corresponding to the 3′ end of the cDNA. Methylene blue–stained rRNAs were the loading control. Numbers refer to transgenic lines.

division. These variables are not necessarily coupled; for example, overexpression of the cyclin-dependent kinase inhibitor *KRP1* or *KRP2* reduced the rate of cell division in young leaves without affecting the moment of cell cycle start and arrest (Wang et al., 2000; De Veylder et al., 2001). In these lines, a similar uncoupling of cell growth from cell division was observed (fewer but larger cells). In the case of the smaller leaves of the *smp*^{epi} mutant, the reduced leaf cell number is attributed to a precocious arrest of cell proliferation, which was inferred from the level of cell vacuolation and cell number of similarly aged leaf primordial.

The *KRP*-overexpressing lines also exhibit a similar leaf morphology change (pronounced serration phenotype at the leaf teeth), which has been attributed to the continuous high expression of mitotic cyclins (*CYCB1;1* and *CYCA2;1*) at the leaf teeth and in the surrounding vasculature during late leaf development when they are turned off in other parts of the leaf (Van Lijsebettens and Clarke, 1998; Burssens et al., 2000). Mitotic cyclin expression reduces *KRP*'s inhibitory effect on cell division activity. The *smp*^{epi} mutation may similarly be less effective at inhibiting cell division activity in the veins that extend to the teeth because vascular cells were least affected by the *smp*^{epi} mutation.

In animals, generally, changes in cell size can be compensated for by changes in cell number to maintain the final size of an organism (reviewed in Day and Lawrence, 2000; Weinkove and Leevers, 2000). Similarly, for plants, alterations in either cell proliferation or cell expansion alone generally do not affect final organ shape nor size, suggesting that some intrinsic patterning mechanism(s) senses the final shape and size and regulates them by altering the other parameter (Hemerly et al., 1995; Smith et al., 1996; Cleary and Smith, 1998; Jones et al., 1998; Wang et al., 2000; De Veylder et al., 2001; Autran et al., 2002). However, several examples suggest that such compensatory mechanisms might not always be activated. For example, overexpression of *ANT* increases not only cell proliferation but also final organ size, and it does this through activation of ectopic *CYCD3;1* expression (Mizukami and Fischer, 2000). Also, overexpression of *E2Fa* and *Dpa*, which encode transcription factors involved in the activation of cell cycle genes, induces extra cell divisions but also severely inhibits overall plant growth in Arabidopsis (De Veylder et al., 2002). Kim and Sinha (2003) suggested that timing may be the critical third dimension that determines whether compensatory mechanisms come into play or not. It may be that these mechanisms are activated when cell proliferation or expansion is altered downstream of cell cycle genes. In the case of *SMP1* and *SMP2*, their effect on the phase duration of cell proliferation in lateral organs is sensed by some intrinsic patterning mechanism(s); the reduced activity of both genes or the increased expression of *SMP1* produces fewer but larger cells or more numerous but smaller cells per area, respectively.

METHODS

Plant Materials and Growth Conditions

Arabidopsis thaliana ecotypes Columbia (Col-0) and Landsberg carrying the *erecta* mutation (L*er*) were used for comparison with mutant plants and for crosses. Seeds were grown under constant white light (~300 μE m^{-2} s^{-1}) either on 0.75% agar media consisting of MS basal salts (Sigma-Aldrich, St. Louis, MO), Haughn and Somerville (1986) nutrient solution, 0.5 g/L Mes, and 10 g/L sucrose or on soil (3:1 mix of Metro-Mix 200 to vermiculite; Scotts, Marysville, OH).

Mutant Isolation

A visual screen for venation pattern mutants was performed on diepoxybutane-mutagenized M2 Arabidopsis (ecotype Col-0) seeds. Briefly, hydrated seeds were incubated in 18 mM diepoxybutane (Sigma-Aldrich) for 4 h and washed extensively before planting (M1 generation). M2 seeds, the progeny of self-fertilized M1 plants, were pooled from every 10 M1 line and screened ~2 weeks after germination. One to two rosette leaves from each M2 plant were fixed in 3:1 ethanol:acetic acid, dehydrated in an ethanol series, cleared in Hemo-De (Fisher Scientific, Fairlawn, NJ), mounted on slides with 2:1 Permount (Fisher Scientific) to xylene, and viewed under dark-field optics for alterations in the venation pattern. Putative venation pattern mutants were confirmed by a secondary screen and backcrossed twice to wild-type Col-0 plants for further phenotypic characterization.

Histochemical Localization of GUS Activity and Histological Analyses

Plant tissues were stained for GUS activity overnight at 37°C in GUS buffer, 20% methanol, and 0.5 mg/mL 5-bromo-4-chloro-3-indolyl-β-D-glucuronidase as described by Malamy and Benfey (1997). For observation of whole mounts, both stained and unstained tissue were fixed, cleared, and mounted on slides as described above. Specimens were

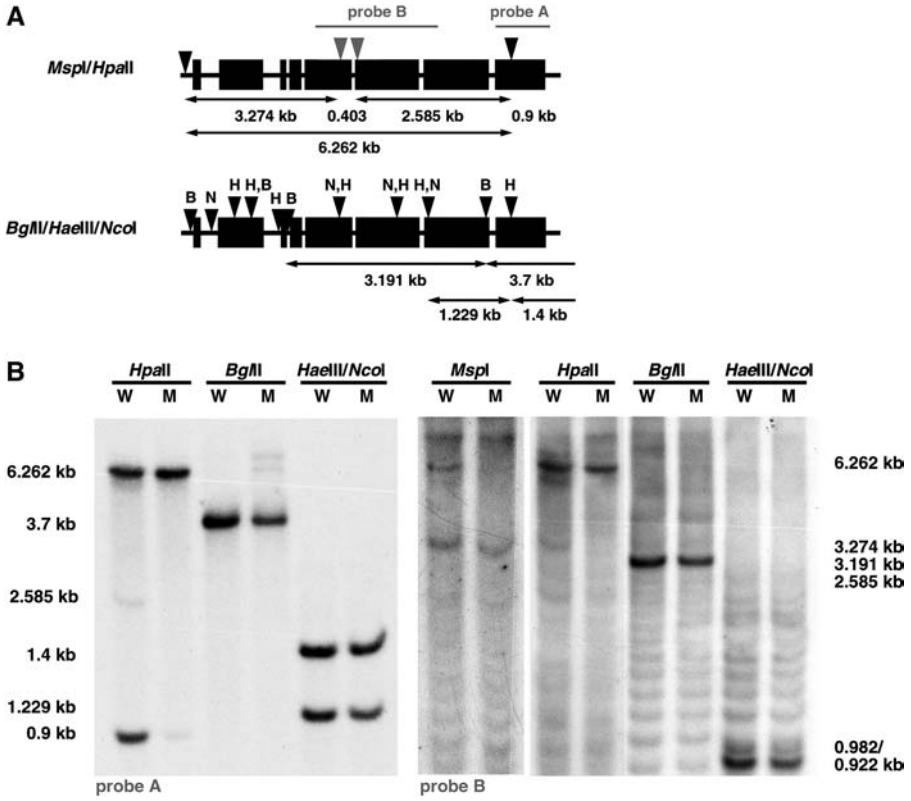

Figure 12. *SWP* Is Hypomethylated in *smp*^{epi}.

(A) Restriction map of *SWP* locus. Black boxes indicate exons, and arrowheads indicate recognition sites of methylation-sensitive enzymes *Bgl*II, *Hae*III, *Nco*I, *Hpa*II, and *Msp*I. Gray arrowheads indicate sites found to be methylated.

(B) DNA gel blots of digested DNA from wild-type (W) and *smp*^{epi} (M) plants were hybridized with either ^{32}P-labeled probe A (left) or ^{32}P-labeled probe B (right). Note the presence and abundance of 6.262-kb band in both *Hpa*II digests and in the *Msp*I digest of wild-type DNA. Also, all three bands (3.274, 2.585, and 2.265 kb) were reduced in the *Hpa*II digest of *smp*^{epi}.

examined with a Zeiss Axiophot microscope (Oberkochen, Germany). Tissues used for RNA in situ hybridizations and scanning electron microscopy were fixed overnight at 4°C in FAA (3.7% formaldehyde, 50% ethanol, and 5% acetic acid). For histological analysis, fixed dehydrated specimens were embedded in Spurr's media (EM Sciences, Ft. Washington, PA) or in Paraplast Plus (Fisher Scientific). Plastic sections (2 μm) were cut on a Sorvall MT2-B ultramicrotome (Newtown, CT) with glass knives and were stained briefly with 1% toluidine blue. Paraffin sections (8 μm) were cut on a model 820 microtome (Arthur H. Thomas Co., Philadelphia, PA). Specimens were prepared for scanning electron microscopy by overnight fixation in 3:1 ethanol:glacial acetic acid, dehydration through an ethanol series, and critical-point drying with liquid carbon dioxide in a Polaron pressure chamber (Watford, Hertfordshire, UK). Dried samples were mounted on stubs, sputter coated with gold-palladium alloy for 30 s or with gold for 2 min, examined with an ISI SS-40 scanning electron microscope (Santa Clara, CA), and photographed on Polaroid Polapan 53 film (Waltham, MA).

Genetic Mapping and Plant Transformation Vector Construction

Plants homozygous for the *smp*^{epi} mutation were crossed to wild-type L*er* plants to generate an F2 mapping population. DNA from 20 mutant plants were used with simple sequence length polymorphic markers (Bell and Ecker, 1993; Ponce et al., 1998) to map the chromosomal location of the *smp*^{epi} mutation, and DNA from ~188 mutant plants were used with Cereon's insertion/deletion and single-nucleotide polymorphism markers (Jander et al., 2002) to finely map the *smp*^{epi} mutation to a region spanned by a single BAC.

The *SMP1* coding sequence along with 810 bp of upstream sequence and 160 bp of downstream sequence were PCR amplified and subcloned into *Xba*I/*Sac*I sites of the PJIM19 (BAR) binary vector. The *SMP1* coding sequence was subcloned into *Bam*HI/*Sac*I sites of the PJIM19 (KAN) binary vector downstream of the *35S CaMV* promoter. Upstream sequence (180 bp) was subcloned into *Xba*I/*Bam*HI sites of the PBI101 binary vector (Clontech, Palo Alto, CA) upstream of the GUS gene. The *SMP1* coding sequence (minus the stop codon) was PCR amplified and subcloned into *Xba*I/*Stu*I sites of the PJIM19smGFP binary vector in frame and upstream of the *smGFP* gene (minus the start codon). All four constructs were sequenced for errors and introduced into wild-type and/or *smp*^{epi} plants via the *Agrobacterium tumefaciens*–mediated floral dip method (Clough and Bent, 1998), and transformants were selected on agar media containing 15 μg/mL BASTA or 50 μg/mL kanamycin.

DNA Gel Blot Analysis

Two micrograms of genomic DNA was digested with *Bgl*II, *Bst*BI, *Cla*I, *Hae*III, *Mbo*I, *Nco*I, *Pst*I, *Pvu*I, *Pvu*II, *Sau3*AI, *Hpa*II, or *Msp*I for 6 h, electrophoresed in 1.5% agarose gel, transferred to ZetaProbe GT

blotting membrane (Bio-Rad, Hercules, CA), UV cross-linked, and baked for 2 h at 80°C. Blots were hybridized to ^{32}P-labeled DNA probes overnight at 42°C, washed twice at 55°C for 10 min in 1× SSC/1% SDS, and exposed to Eastman Kodak X-OMAT AR film (Rochester, NY) at −70°C.

Total RNA Isolation and RNA Gel Blot Analysis

Total RNA was isolated from the aerial part of 38-d-old plants with TRIzol (Gibco BRL, Cleveland, OH) according to the manufacturer's instructions. Ten micrograms of total RNA was electrophoresed in 1.2% formaldehyde-agarose gel, transferred to ZetaProbe GT blotting membrane (Bio-Rad), UV cross-linked, and baked for 2 h at 80°C. Blots were stained with 0.02% methylene blue/0.3 M sodium acetate, pH 5.2, for 3 min, and destained with 20% ethanol for 10 to 15 min, and the resulting rRNA bands were visualized with a Gel Doc 2000 (Bio-Rad). Blots were then hybridized to ^{32}P-labeled DNA probes overnight at 42°C, washed at 55°C for 30 min in 1× SSC/1% SDS and then in 0.5× SSC/2.5% SDS, and exposed to Eastman Kodak X-OMAT AR film at −70°C.

RT-PCR

Two micrograms of total RNA was reverse-transcribed with 200 units of Superscript II (Invitrogen, Carlsbad, CA). The resulting cDNA:RNA hybrids were treated with 10 units of DNase I (Roche, Indianapolis, IN) for 30 min at 37°C, purified on Qiaquick PCR column (Qiagen, Valencia, CA), and used as template to PCR amplify *SMP1* (40 cycles), *SMP2* (40 cycles), *SWP* (40 cycles), and *eIF4A* (39 cycles). PCR conditions are as follows: 94°C for 15 s, 52°C for 15 s, and 72°C for 20 s. PCR products (350 to 440 bp) were electrophoresed in 1.5% agarose gel and visualized with a Gel Doc 2000. Primer sequences for *SMP1* are 5′-GACCATAGGAAGCAAATTGA-3′ and 5′-AAGATCTATCACACGATGGT-3′; for *SMP2* are 5′-GATCACAGGAAGAAATTAGAA-3′ and 5′-ACGATCTACCACATGACGGT-3′; and for *SWP* are 5′-TCTGCTCTTGTTGGTCGAG-3′ and 5′-TGATAAGAACCTGTCAGCAA-3′.

RNA in Situ Hybridization

SMP1 cDNA (nucleotides 439 to 640 relative to ATG) was PCR amplified with primers containing engineered T7 and T3 RNA polymerase promoter sites and used as template to generate dioxigenin-labeled sense and antisense RNA probes. In situ hybridizations and labeling reactions were performed as described by Jackson (1991) with some modifications, which were described by Clay and Nelson (2002).

Cell Counts

For each genotype, transverse sections through a total of three adult leaves were used for cell counts per defined area. The defined area encompassed a region just right or left of the midvein, and the average of two serial sections was used to calculate the mean cell number per area for each leaf. This average was then used to calculate the mean cell number per area for all three leaves.

ACKNOWLEDGMENTS

Sequencing analysis was performed by the HHMI Biopolymer/Keck Foundation Biotechnology Resource Lab (Yale University, New Haven, CT). We thank James A. Sullivan for his generous gift of the PJIM19 vectors. This work was supported by National Science Foundation Grants IBN-0114648 and IBN-0416731 to T.N.

Received March 18, 2005; revised May 9, 2005; accepted May 12, 2005; published June 3, 2005.

REFERENCES

Ach, R.A., Durfee, T., Miller, A.B., Taranto, P., Hanley-Bowdoin, L., Zambryski, P., and Gruissem, W. (1997). *RRB1* and *RRB2* encode maize retinoblastoma-related proteins that interact with a plant D-type cyclin and geminivirus replication protein. Mol. Cell. Biol. **17,** 5077–5086.

Alonso, J.M., et al. (2003). Genome-wide insertional mutagenesis of *Arabidopsis thaliana*. Science **301,** 653–657.

Autran, D., Jonak, C., Belcram, K., Beemster, G.T.S., Kronenberger, J., Grandjean, O., Inzé, D., and Traas, J. (2002). Cell numbers and leaf development in *Arabidopsis*: A functional analysis of the *STRUWWELPETER* gene. EMBO J. **21,** 6036–6049.

Bell, C.J., and Ecker, J.R. (1993). Assignment of 30 microsatellite loci to the linkage map of *Arabidopsis*. Genomics **19,** 137–144.

Boger-Nadjar, E., Vaisman, N., Ben-Yehuda, S., Kassir, Y., and Kupiec, M. (1998). Efficient initiation of S-phase in yeast requires Cdc40p, a protein involved in pre-mRNA splicing. Mol. Gen. Genet. **260,** 232–241.

Burssens, S., de Almeida Engler, J., Beeckman, T., Richard, C., Shaul, O., Ferreira, P., Van Montagu, M., and Inzé, D. (2000). Developmental expression of the *Arabidopsis thaliana* CycA2;1 gene. Planta **211,** 623–631.

Chawla, G., Sapra, A.K., Surana, U., and Vijayraghavan, U. (2003). Dependence of pre-mRNA introns on *PRP17*, a non-essential splicing factor: Implications for efficient progression through cell cycle transitions. Nucleic Acids Res. **31,** 2333–2343.

Chua, K., and Reed, R. (1999). Human step II splicing factor hSlu7 functions in restructuring the spliceosome between the catalytic steps of splicing. Genes Dev. **13,** 841–850.

Clay, N.K., and Nelson, T. (2002). *VH1*: A provascular-specific receptor kinase that influences leaf cell patterns in Arabidopsis. Plant Cell **14,** 2707–2722.

Cleary, A.L., and Smith, L.G. (1998). The *Tangled1* gene is required for spatial control of cytoskeletal arrays associated with cell division during maize leaf development. Plant Cell **10,** 1875–1888.

Clough, S.J., and Bent, A.F. (1998). Floral dip: A simplified method for *Agrobacterium*-mediated transformation of *Arabidopsis thaliana*. Plant J. **16,** 735–743.

Curtis, D., Treiber, D.K., Tao, F., Zamore, P.D., Williamson, J.R., and Lehmann, R. (1997). A CCHC metal-binding domain in Nanos is essential for translational regulation. EMBO J. **16,** 834–843.

Day, S.J., and Lawrence, P.A. (2000). Measuring dimensions: The regulation of size and shape. Development **127,** 2977–2987.

De Veylder, L., Beeckman, T., Beemster, G.T.S., de Almeida Engler, J., Ormenese, S., Maes, S., Naudts, M., Van der Schueren, E., Jacqmard, A., Engler, G., and Inzé, D. (2002). Control of proliferation, endoreduplication and differentiation by Arabidopsis E2Fa-Dpa transcription factor. EMBO J. **21,** 1360–1368.

De Veylder, L., Beeckman, T., Beemster, G.T.S., Krols, L., Terras, F., Landrieu, I., Van der Schueren, E., Maes, S., Naudts, M., and Inzé, D. (2001). Functional analysis of cyclin-dependent kinase inhibitors of Arabidopsis. Plant Cell **13,** 1653–1667.

Dewitte, W., Riou-Khamlichi, C., Scofield, S., Healy, J.M.S., Jacqmard, A., Kilby, N.J., and Murray, J.A.H. (2003). Altered cell cycle distribution, hyperplasia, and inhibited differentiation in Arabidopsis caused by the D-type cyclin CYCD3. Plant Cell **15,** 79–92.

Donnelly, P.M., Bonetta, D., Tsukaya, H., Dengler, R.E., and Dengler,

N. (1999). Cell cycling and cell enlargement in developing leaves of Arabidopsis. Dev. Biol. **215,** 407–419.

Doonan, J. (2000). Social controls on cell proliferation in plants. Curr. Opin. Plant Biol. **3,** 482–487.

Frank, D., and Guthrie, C. (1992). An essential splicing factor, SLU7, mediates 3′ splice site choice in yeast. Genes Dev. **6,** 2112–2124.

Grandjean, O., Vernoux, T., Laufs, P., Belcram, K., Mizukami, Y., and Traas, J. (2004). In vivo analysis of cell division, cell growth, and differentiation at the shoot apical meristem in Arabidopsis. Plant Cell **16,** 74–87.

Guo, K., and Walsh, K. (1997). Inhibition of myogenesis by multiple cyclin-Cdk complexes. Coordinate regulation of myogenesis and cell cycle activity at the level of E2F. J. Biol. Chem. **272,** 791–797.

Hansen, L.J., Chalder, D.L., and Sandmeyer, S.B. (1988). Ty3, a yeast retrotransposon associated with tRNA genes, has homology to animal retroviruses. Mol. Cell. Biol. **3,** 5245–5256.

Haughn, G.W., and Somerville, C. (1986). Sulfonylurea-resistant mutants of *Arabidopsis thaliana*. Mol. Gen. Genet. **204,** 430–434.

Hemerly, A., de Almeida Engler, J., Van Montagu, M., Engler, G., Inzé, D., and Ferreira, P. (1995). Dominant negative mutants of the Cdc2 kinase uncouple cell division from iterative plant development. EMBO J. **14,** 3925–3936.

Hemerly, A.S., Ferreira, P.C.G., de Almeida Engler, J., Van Montagu, M., Engler, G., and Inzé, D. (1993). *cdc2a* expression in *Arabidopsis thaliana* is linked with competence for cell division. Plant Cell **5,** 1711–1723.

Hwang, L.H., and Murray, A.W. (1997). A novel yeast screen for mitotic arrest mutants identifies *DOC1*, a new gene involved in cyclin proteolysis. Mol. Biol. Cell **10,** 1877–1887.

Jackson, D. (1991). In-situ hybridisation in plants. In Molecular Plant Pathology: A Practical Approach, D.J. Bowles, J.S.J. Gurr, and M. McPherson, eds (Oxford: Oxford University Press), pp. 163–174.

Jacobsen, S.E., and Meyerowitz, E.M. (1997). Hypermethylated *SUPERMAN* epigenetic alleles in *Arabidopsis*. Science **277,** 1100–1103.

Jander, G., Norris, S.R., Rounsley, S.D., Bush, D.F., Levin, I.M., and Last, R.L. (2002). Arabidopsis map-based cloning in the post-genome era. Plant Physiol. **129,** 440–450.

Jones, A.M., Im, K.-H., Savka, M.A., Wu, M.-J., DeWitt, G., Shillito, R., and Binns, A.N. (1998). Auxin-dependent cell expansion mediated by overexpressed auxin-binding protein 1. Science **282,** 1114–1117.

Kim, M., and Sinha, N. (2003). Regulating shapes and sizes. Dev. Cell **4,** 441–447.

Luff, B., Pawlowski, L., and Bender, J. (1999). An inverted repeat triggers cytosine methylation of identical sequences in *Arabidopsis*. Mol. Cell **3,** 505–511.

Malamy, J.E., and Benfey, P.N. (1997). Organization and cell differentiation in lateral roots of *Arabidopsis thaliana*. Development **124,** 33–44.

Martinez, M.C., Jørgensen, J.-E., Lawton, M.A., Lamb, C.J., and Doerner, P.W. (1992). Spatial pattern of *cdc2* expression in relation to meristem activity and cell proliferation during plant development. Proc. Natl. Acad. Sci. USA **89,** 7360–7364.

McDonald, W.H., Ohi, R., Smelkova, N., Frendewey, D., and Gould, K.L. (1999). Myb-related fission yeast cdc5p is a component of a 40S snRNP-containing complex and is essential for pre-mRNA splicing. Mol. Cell. Biol. **19,** 5352–5362.

Mizukami, Y., and Fischer, R.L. (2000). Plant organ size control: *AINTEGUMENTA* regulates growth and cell numbers during organogenesis. Proc. Natl. Acad. Sci. USA **97,** 942–947.

Mount, S.M., and Rubin, G.M. (1985). Complete nucleotide sequence of the *Drosophila* transposable element copia: Homology between copia and retroviral proteins. Mol. Cell. Biol. **5,** 1630–1638.

Ponce, M.R., Quesada, V., and Micol, J.L. (1998). Rapid discrimination of sequences flanking and within T-DNA insertions in the Arabidopsis genome. Plant J. **14,** 497–501.

Rajavashisth, T.B., Taylor, A.K., Andalibi, A., Svenson, K.L., and Lusis, A.J. (1989). Identification of a zinc finger protein that binds to the sterol regulatory element. Science **245,** 640–643.

Roussell, D.L., and Bennett, K.L. (1993). glh-1, a germ-line putative RNA helicase from *Caenorhabditis*, has four zinc fingers. Proc. Natl. Acad. Sci. USA **90,** 9300–9304.

Schwartz, D.E., Tizard, R., and Gilbert, W. (1983). Nucleotide sequence of rous sarcoma virus. Cell **32,** 853–869.

Shea, J.E., Toyn, J.H., and Johnston, L.H. (1994). The budding yeast U5 snRNP Prp8 is a highly conserved protein which links RNA splicing with cell cycle progression. Nucleic Acids Res. **22,** 5555–5564.

Shinnick, T.M., Lerner, R.A., and Sutcliffe, J.G. (1981). Nucleotide sequence of Moloney murine leukaemia virus. Nature **342,** 543–548.

Skapek, S.X., Rhee, J., Spicer, D.B., and Lassar, A.B. (1995). Inhibition of myogenic differentiation in proliferating myoblasts by cyclin D1-dependent kinase. Science **267,** 1022–1024.

Smith, L.G., Hake, S., and Sylvester, A.W. (1996). The *tangled-1* mutation alters cell division orientations throughout maize leaf development without affecting leaf shape. Development **122,** 481–489.

Stam, M., Belele, C., Dorweiler, J.E., and Chandler, V.L. (2002). Differential chromatin structure within a tandem array 100 kb upstream of the maize *b1* locus is associated with paramutation. Genes Dev. **16,** 1906–1918.

Stöger, R., Kubicka, P., Liu, C.-G., Kafri, T., Razin, A., Cedar, H., and Barlow, D.P. (1993). Maternal-specific methylation of the imprinted mouse *Igf2r* locus identifies the expressed locus as carrying the imprinted signal. Cell **73,** 61–71.

Vaisman, N., Tsouladze, A., Robzyk, K., Ben-Yehuda, S., Kupiec, M., and Kassir, Y. (1995). The role of *Saccharomyces cerevisiae* Cdc40p in DNA replication and mitotic spindle formation and/or maintenance. Mol. Gen. Genet. **247,** 123–136.

Van Lijsebettens, M., and Clarke, J. (1998). Leaf development in *Arabidopsis*. Plant Physiol. Biochem. **36,** 47–60.

Wain-Hobson, S., Sonigo, P., Danos, O., Cole, S., and Alizon, M. (1985). Nucleotide sequence of the AIDS virus, LAV. Cell **40,** 9–17.

Wang, H., Zhou, Y., Gilmer, S., Whitwill, S., and Fowke, C.L. (2000). Expression of the plant cyclin-dependent kinase inhibitor ICK1 affects cell division, plant growth and morphology. Plant J. **24,** 613–623.

Weinkove, D., and Leevers, S.J. (2000). The genetic control of organ growth: Insights from *Drosophila*. Curr. Opin. Genet. Dev. **10,** 75–80.

Zachsenhaus, E., Jiang, Z., Chung, D., Martin, J.D., Phillips, R.A., and Gallie, B.L. (1996). pRb controls proliferation, differentiation, and death of skeletal muscle cells and other lineages during embryogenesis. Genes Dev. **10,** 3051–3064.

Zhang, P., Wong, C., DePinho, R.A., Harper, J.W., and Elledge, S.J. (1998). Cooperation between the Cdk inhibitors p27(KIP1) and p57(KIP2) in the control of tissue growth and development. Genes Dev. **12,** 3162–3167.